Hindawi
Journal of Engineering
Volume 2023, Article ID 1943535, 19 pages
https://doi.org/10.1155/2023/1943535

Research Article

Dual Strategy of Reconfiguration with Capacitor Placement for Improvement Reliability and Power Quality in Distribution System

Ali Nasser Hussain,[1] **Wathiq Rafa Abed**,[2] **and Mohanad Muneer Yaqoob**[1]

[1]*Middle Technical University, Electrical Engineering Technical College, Department of Electrical Power Engineering Techniques, Baghdad, Iraq*
[2]*Middle Technical University, Institute of Technology, Electrical Power Department, Baghdad, Iraq*

Correspondence should be addressed to Mohanad Muneer Yaqoob; bcc0037@mtu.edu.iq

Received 26 October 2022; Revised 21 January 2023; Accepted 13 February 2023; Published 15 March 2023

Academic Editor: Yuh Shyan Hwang

The demand for electrical power has been increasing rapidly due to higher industrial output and deregulation. The concerns have been raised about the ability of distribution networks to provide adequate power for the customers with an appropriate level of quality and reliability. To ameliorate the performance of the radial distribution system (RDS), the optimal capacitor placement (OCP), and the distribution system reconfiguration (DSR) strategies have been implemented in the current work to achieve the highest power quality and system reliability in a balanced manner at the same time. Three different scenarios were implemented, the first scenario of dual sequential (OCP after DSR), the second scenario of dual sequential (DSR after OCP), and the third scenario of dual simultaneous (DSR with OCP). These scenarios were tested on typical 33 and 69 bus IEEE RDS using the binary salp swarm algorithm (BSSA) based on the multiobjective functions (MOFs), in order to identify the most effective scenario performance that achieved the highest power quality and system reliability. The MOF was formulated to improve the power quality by increasing the voltage buses and reducing the power losses. While the constraints include limits of system reliability indices to provide optimal constraints on negative interactions of power quality. The simulation results demonstrate that the second scenario of dual sequential (DSR after OCP) provide superior in comparison with the first scenario of dual sequential (OCP after DSR) for enhancing the RDS reliability indices, voltage buses, and reducing power losses. Finally, the best result can be realized with dual simultaneous (DSR and OCP) in the third scenario compared to the dual sequential scenarios.

1. Introduction

Distribution system failures cause 80% of all consumer outages, according to utility data. Moreover, the majority of customers are linked at the level of distribution, which represents the highest proportion of investment expenditures. Consequently, enhancing the reliability of RDS leads to raising the chances of the overall electrical power system to operate without failure. Therefore, efficient computing methodologies are required to assess the reliability of RDS [1, 2].

The electrical network operator needs to provide electric power to the consumers while maintaining suitable levels of reliability and keeping the node voltages within allowable limits [3]. To reduce the fault currents and an efficient configuration of protective devices, the distribution system (DS) is built as a radial structure [4, 5]. RDS is reconfigured utilizing the normally open (N.O), as well as normally close (N.C) switches to establish the radial limitation, which improves overall performance [6, 7]. Numerous issues with RDS, including increased active losses, bus voltage variations, overloading, and off-balance loads can be resolved by utilizing a variety of ways. The following methods are suggested for resolving the aforementioned RDS issues: distributed generation (DG), OCP, and DSR [8–10].

In conjunction with increased the demand for electric power, the scarcity of fossil fuel resources with its high costs,

as well as the environmental problems resulting from it such as global warming for example. So, the need to preserve the environment by reducing air pollution is essential [11–13]. This explained why the OCP and DSR techniques have been an important topic for researchers in the recent years. The ability of capacitors to provide the reactive power has contributed to the improvement of the voltage profile and power factor and thus reduced the losses. So, the optimal placement of capacitors in DS is one of the important things nowadays. Depending on how and where the capacitors are positioned in the system, the advantages of this sort of correction may vary [14–17]. Also, the RDS reconfiguration technique is presented as the most economical strategy because the installation and operating costs for DG or capacitors are not included [18]. The optimal solutions for these problems are solved using artificial intelligence and optimization-based algorithms. Moreover, the OCP and DSR have been subjected to numerous studies, and various approaches with various objective functions have been used to model the network and address the problems using optimization algorithms such as improved particle swarm optimization (IPSO), grey wolf optimization (GWO), and flower pollination algorithm (FPA) [19–21].

Sudhakara and Reddy for the best placement of DSR published a metaheuristic optimization method that depends on the whale optimization algorithm (WOA) in IEEE DS using 33 and 119 buses. The DSR problem was solved using the WOA algorithm. This method provides a high voltage for the buses despite having small active power losses of 139.5697 kW, which is utilized to lower active losses and raise the voltage for each bus in the standard networks [22]. Furthermore, Diab and Rezk used a new optimization algorithm to detect the OCP and DSR using dragonfly optimization (DFO), GWO, and moth-flame algorithm (MFA). In this work, the performance and efficiency of these algorithms are validated using 33, 69, and 118-bus IEEE systems. Also, the MATLAB/Simulink software was used to assess the convergence performance for tested RDSs [23]. Chakrabarti et al. presented a DSR technique which maximizes the reliability of IEEE 13-bus RDS using the binary PSO algorithm that is used to determine the optimal configuration of switches in the network. The reliability is calculated by using the Monte Carlo simulation technique [24]. Sedighizadeh et al. presented a new approach based on the dual and simultaneous of DSR and OCP technologies with a usual optimization process of improving the binary PSO. This method has been tested for 16 and 33 bus RDSs to improve the voltage profile and reduce active losses [25]. Reddy and Reddy have applied a sequential approach to solving DSR and OCP problems. Ant line optimization algorithm (ALO) is used to find the best OCP size and location for RDS after implementing the DSR technique. The test was conducted to reduce active loss and improve saving on the two IEEE-33 and IEEE-69 RDS. The results demonstrate the success of the proposed approach in which the active power losses are reduced by 44.97% and 67.31% when the OCP is installed for the reconfigured network of 33 buses and 69 buses, respectively, and the net savings are increased to 82,944 $ and 75,456 $ [26]. Gallego et al. introduced the mixed linear programming (MILP) model for simultaneous DSR and OCP solution in RDS. This optimization process is carried out in order to reduce the overall cost, reduce active loss, and optimize the voltage profile. This approach is applied to IEEE-(33, 69, 83, 119, 136, 202, and 417) bus RDSs. The optimal result obtained via this technique demonstrated that the simultaneous technique of optimal DSR with OCP is able to improve the voltage profile and reduce both total and capacitor costs. Also, the results show the active loss percentage reduced to 54.28%, 68.93%, 30.81%, 46.95%, 21.12%, 26.65%, and 27.90%, respectively, for the RDSs that were used in this test [27]. However, the previous studies had a number of drawbacks, where many of these papers focused on the improvement of power quality or reliability that dealt with separately from others. For example, Tamilselvan et al. presented a single objective function to reduce the losses for RDS, while neglecting to include the improvement of voltage profile and system reliability as well [28]. In contrast, other researchers presented several studies to improve the reliability individually without paying attention to the effect of power quality.

As a result to avoid these drawbacks, the current work presented a new study in which the improvement process considers both aspects of the power quality and reliability of RDS together. The optimization process has been carried out in a balanced manner, where reducing the total losses and enhancing the voltage profile for the distribution system are included as a MOF, and the improvement of reliability was also included as a constraint and a prerequisite for the optimization process.

In this study, three scenarios for dual sequentially OCP after DSR, DSR after OCP, and dual-simultaneous DSR and OCP based on the BSSA optimization method were implemented on 33 and 69 IEEE buses RDS. Therefore, the best capacitor placement, size, and optimum structure of RDS are chosen to reduce the active losses and improve voltage for all buses with a comprehensive enhancement of system reliability using this optimization method. Moreover, MATLAB software environmental is used to test the presented RDS with using the m-file function tool.

2. Materials and Methods

The load flow, MOF, reliability assessment, RDS constraints, and BSSA algorithm that applied in this study are described and explained in detail in this section.

2.1. Load Flow Analysis for RDS. The distribution networks use conductors that have a high ratio of R/X, a radial construction with many nodes (buses), branches, DG, and complicated topology configurations that can be altered for repair tasks and contingency operations [17, 29]. Also, the ability of load flow techniques to perform the calculations relating for RDS such as current, voltage, active power losses, and total cost has enhanced their significance recently.

Due to RDS radial construction, high resistance to reactance ratio, and imbalanced nature of the loads, standard approaches were unable to provide quick convergence for

load flow solution. The backward/forward sweep technique was created and published [30]. However, when applied the computer code of the backward/forward sweep algorithm, the authors did not clarify how determined each branch end in automatically form or where to begin the backward computation. The answer is found by straightforward matrix multiplication of the two matrices bus injection to bus current (BIBC) and bus current to bus voltage (BCBV), which were developed from the network topological structure as part of a direct technique of backward/forward sweep reported in reference [31]. The next three crucial stages are defined beginning at the terminal node, while taking into account the electrical properties shown in Figure 1.

Step 1 (computation of the nodal current): by using equation (1), the current injection at each node (i) can be obtained as follows [31]:

$$I_i^{(k)} = \text{conj}\left(\frac{P_{n-i} + j * Q_{n-i}}{V_{n-i}^{(k)}}\right), i = 1, 2, 3, \cdots, n, \quad (1)$$

where P_{n-i} and Q_{n-i} are active and reactive power injection at node i, respectively, and the node voltage $V_{n-i}^{(k)}$.

Step 2 (backward sweep): beginning with the last branch, the current (J_{i+1}) for any branch from node (i) to the node $(i+1)$ is calculated from equation (2) as follows:

$$J_{n-i}^{(k)} = -\text{conj}\left(\frac{P_{n-i} + j * Q_{n-i}}{V_{n-i}^{(k)}}\right) + \sum_r J_{n-r}^{(k)}\ r = 1, \quad (2)$$

where $\sum_r J_{n-r}^{(k)}$ represents current in branches coming from node (i).

Step 3 (forward sweep): using equation (3), the node adjusted voltages beginning at the root bus.

$$V_i^{(k)} = V_{i-1}^{(k)} - Z_i J_i^{(k)}, i = 1, 2, \cdots, n, \quad (3)$$

where Z_i symbolize the impedance of the branch.

The aforementioned three processes are repeated until the voltage levels in all nodes at the current iteration and the preceding fall below a tolerance limit ε.

$$\left(V^{K+1}\right) - \left(V^K\right) < \varepsilon. \quad (4)$$

2.2. Objective Function. Figure 2 shows the MOF schematic used in this study. The MOF was formulated to minimize the active power losses and maximize the voltage profile. The MOF is used in this instance to achieve the best OCP and DSR in the RDS.

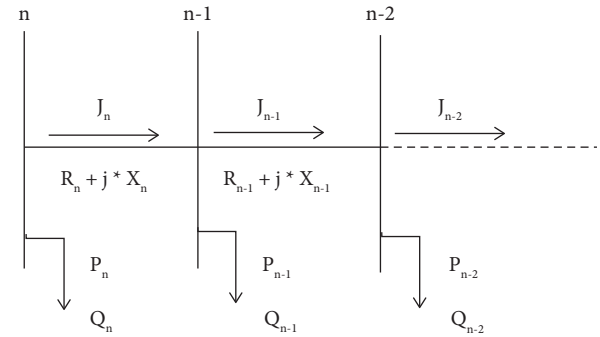

Figure 1: The load flow analysis in RDS.

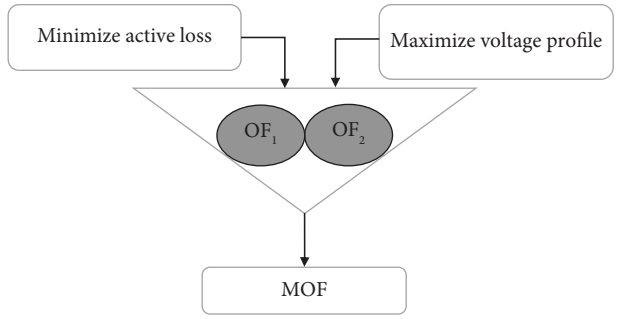

Figure 2: The MOF diagram.

The MOF can be represented as the following equations [32]:

$$OF_1 = \text{Minimize } P_{T,L},$$
$$P_{T,L} = \sum_{a=1}^{N_b} P_{L,a} KW, \quad (5)$$
$$P_{L,a} = I_a^2 * R_a KW,$$

where $P_{T,L}$, $P_{L,a}$, N_b, I_a, and R_a represent the total real power loss, the loss per branch a, number of branches, flow of current in branch a, and resistance of branch a.

To enhancement the voltage profile, the voltage must stay within normal limits.

$$OF_2 = V_G * r_{e_v} + C_G * r_{e_i}, \quad (6)$$

where V_G, C_G, r_{e_v}, and r_{e_i} represent consecutively bus voltage limits, current of branch limits, penalty factor for bus voltage (when the bus voltage is within permissible limits, this factor equals 0), and penalty factor for branch current (if the branch current does not exceed the thermal limit, this equals 0).

Therefore,

$$MOF = OF_1 + OF_2. \quad (7)$$

2.3. Reliability Assessment. The word reliability refers to a system's ability to execute its intended purpose, i.e., analysis of the ability of the distribution system to meet the needs of load [33]. The reliability evaluation of the entire network is based on the reliability of each part included in this network which has two states, either an operating state or a failed state. This enables to distinct the network state by identifying the state of components. The failure probability of power system components owing to outages of lines, transformers, and generators may be used to calculate the system's reliability. A line, transformer, and generator outage may have more than one failure condition so the reliability analysis of RDS is of high importance for continuous operation [34].

Different reliability indices can be used to represent the results of a reliability study. Reliability indices are used to assess the degree or relevance of a system outage [33]. To execute the reliability evaluation, a suitable set of indices must be determined based on the application. It is generally typical practice in the electric utility business to measure and assess reliability performance using standard IEEE reliability indices. The amount of outage length, repetition of outages, availability of a system, and reaction time are among the reliability indices. The reliability indices standard deviation informs distribution engineers about the expected range of yearly values.

Three fundamentals load point indices may be used to computation the indices of reliability for RDS as the following [35]:

(1) Average failure rate at load point (i), λ_i which is written as following equation (8):

$$\lambda_i = \sum_{j \epsilon N_e} \lambda_{e,j}, \quad (8)$$

where N_e represents the total number of elements whose fault would interrupt load point (i) and $\lambda_{e,j}$ represents the average failure rate at load point (i).

(2) Annual outage duration at load point (i), U_i (an hour per year):

$$U_i = \sum_{j \epsilon N_e} \lambda_{e,j} \bullet r_{i,j}, \quad (9)$$

where $r_{i,j}$ is failure duration at load point (i) owing to a failed element j.

(3) Average outage duration at load point (i), $\mathbf{r}_i$ (hours) as follows:

$$r_i = \frac{U_i}{\lambda_i}. \quad (10)$$

Typically, a measure of RDS reliability is considered as the effects of a prolonged interruption in terms of the number of users disconnected by an outage. The equations are used to compute sustained interruption indices [36–38].

(i) SAIDI: system average interruption duration index.

$$\text{SAIDI} = \frac{\text{Total duration of all interruption}}{\text{Total number of customers connected}},$$
$$\text{SAIDI} = \frac{\sum_{i=1}^{k} U_i N_i}{\sum_{i=1}^{k} N_i}, \left(\frac{h_r}{C \bullet y_r}\right). \quad (11)$$

(ii) SAIFI: system average interruption frequency index.

$$\text{SAIFI} = \frac{\text{Total number of all interruptions}}{\text{Total number of customers connected}},$$
$$\text{SAIFI} = \frac{\sum_{i=1}^{k} \lambda_i N_i}{\sum_{i=1}^{k} N_i} \left(\frac{f}{C \bullet y_r}\right). \quad (12)$$

(iii) CAIDI: customer average interruption duration index.

$$\text{CAIDI} = \frac{\text{Total duration of all interruption}}{\text{Total number of all interruptions}},$$
$$\text{CAIDI} = \frac{\sum_{i=1}^{k} U_i N_i}{\sum_{i=1}^{k} \lambda_i N_i} (h_r). \quad (13)$$

(iv) ASAI: average service availability index.

$$\text{ASAI} = \frac{\text{Total number of hours availability}}{\text{Total demand hours}},$$
$$\text{ASAI} = \frac{\sum_{i=1}^{k} 8760\, N_i - \sum_{i=1}^{k} U_i N_i}{\sum_{i=1}^{k} 8760\, N_i} (p.u.). \quad (14)$$

(v) EENS: expected energy not supplied.

$$\text{EENS} = \sum_{i=1}^{k} p_i U_i \left(\frac{MWhr}{y_r}\right), \quad (15)$$

where p_i represent the average load for load point i

(vi) AENS: average energy not supplied.

$$\text{AENS} = \frac{\text{Total enerage not supplie}}{\text{Total number of customers connected}},$$
$$\text{AENS} = \frac{\sum_{i=1}^{k} \text{EENS}}{\sum_{i=1}^{k} N_i} \left(\frac{MWhr}{C \bullet y_r}\right). \quad (16)$$

(vii) Average service unavailability index (ASUI).

$$\text{ASUI} = 1 - \text{ASAI}\,(\text{p.u.}). \quad (17)$$

2.4. Power Flow and Reliability Assessment Constraints. The following is a description of the power flow and reliability assessment procedure time constraints:

2.4.1. Capacitor Size. The capacitor bank is injected maximum value reactive power into the RDS it should not be above the entire reactive power load and indicated by the following equation (18) [32, 39]:

$$Q_{C,\mathrm{MAX}} < Q_L, \tag{18}$$

where $Q_{C,\mathrm{MAX}}$ is the maximum needed of reactive power amount from capacitor bank in KVAR and Q_L is the all reactive power for a load of the network. However, in the optimal design of the OCP technique, the size of capacitors in the RDS is very important and it must be less than Q_L.

2.4.2. Voltage and Current Limit. This limitation is used to ensure that the voltage value of each bus keeps within the required tolerances based on the following equation (19):

$$V_{\mathrm{MIN}} \le V_i \le V_{\mathrm{MAX}}, \tag{19}$$

where the allowable values of node voltage limited by $V_{\max}$ = 1.05p.u and $V_{\min}$ = 0.95p.u.

However, the current at each brunch must be limited as shown in equation (20) as follows:

$$\left|I_i\right| \le I_{i,\max}. \tag{20}$$

2.4.3. Reliability Constraints. Reliability indices after the optimization process must be better than the base case, as shown in equations as follows:

$$\begin{aligned} 0 < SAIDI < (SAIDI)_B,\\ 0 < SAIFI < (SAIFI)_B,\\ 0 < CAIDI < (CAIDI)_B,\\ 0 < AENS < (AENS)_{\mathrm{B}},\\ ASAI > (ASAI)_B,\\ 0 < EENS > (EENS)_B,\\ 0 < ASUI > (ASUI)_B, \end{aligned} \tag{21}$$

where $(SAIDI)_B$, $(SAIFI)_B$, $(CAIDI)_B$, $(AENS)_B$, $(ASAI)_B$, and $(ASUI)_B$ represent the indices in the base case, and SAIDI, SAIFI, CAIDI, AENS, ASAI, and ASUI are indices after optimization [37].

2.5. Optimization-Based BSSA. In 2017, Mirjalili et al. [40] proposed the SSA where this algorithm depends on the navigation and foraging behavior in the seas and oceans as shown in Figure 3. To update the leader location, the following equation (22) is presented [41]:

$$X_j^1 = \begin{cases} F_j + C_1\left(\left(ub_j - lb_j\right)C_2 + lb_j\right), C_3 \ge 0.5,\\ F_j - C_1\left(\left(ub_j - lb_j\right)C_2 + lb_j\right), C_3 < 0.5, \end{cases} \tag{22}$$

where X_j^1 represents the first location of salp in the j^{th} dimension, F_j represents the location of food supply, ub_j, lb_j are the upper and lower bounds of j^{th} dimension, and the random numbers are denoted by C_2 and C_3 [0, 1]. While the coefficient C_1 is written using the following equation (23):

$$C_1 = 2 \times e^{-(4t/T)^2}, \tag{23}$$

where t represents the present iteration and T is the total number of iterations. The location of the followers can be written as equation (24) [42] as follows:

$$X_j^n = \frac{1}{2}\left(X_j^n + X_j^{n-1}\right), \tag{24}$$

where $n \ge 2$ and X_j^n is the site of n^{th} follower in j dimension.

The salp population is seen as a binary bound of dimension in a binary search issue. The velocity and position values for each particle must be limited to (0 or 1) in order for this method to search in discrete space. So that, the transfer function T.F may be applied as follows [43]:

$$T.F\left(X_j^n(t)\right) = \frac{1}{\left(1 + e^{-X_j^n(t)}\right)}. \tag{25}$$

By using T.F, (24) will be changed to as follows:

$$X_j^d(t+1) = \begin{cases} 0 \ if \ \mathrm{rand} < T.F\left(X_j^d(t+1)\right),\\ 1 \ if \ \mathrm{rand} \ge T.F\left(X_j^d(t+1)\right), \end{cases} \tag{26}$$

where $X_j^d(t+1)$ is the $j-$th element at d^{th} dimension in X solution.

The proposed BSSA is implemented to find the optimal size and location of OCP and optimal topology of DSR that reduces the real power losses, and enhance the voltage profile and reliability. The switches of RDS are represented here as discrete values, where 0 denotes an open switch and 1 denotes a closed switch. The BSSA was carried out which depend on the following steps: (Algorithm 1).

3. Results and Discussion

The MATLAB environment software was used to do the suggested BSSA algorithm for two IEEE standard test systems. The first is 33-bus RDS with 3715 kW, 2300 kVA, and 37 branches with (32 closed and 5 opened switches) as illustrated in Figure 4. The second test system is 69-bus RDS with 100 MVA, 3.8015 MW, 2.6946 MVAr, and 12.66 kV containing 73 branches. The system included, 5 opened tie switches and 68 closed sectionalizing switches as shown in Figure 5. The reliability and line bus data are obtained from references [3, 37] for both systems, respectively. Three scenarios were used to evaluate the effectiveness of the suggested techniques:

Scenario 1: sequentially (OCP after DSR)

Scenario 2: sequentially (DSR after OCP)

Scenario 3: simultaneously (DSR and OCP)

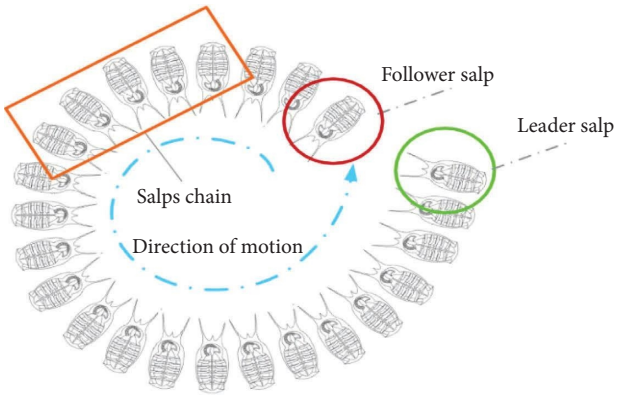

Figure 3: Chain of SSA.

(1) Initialize the search agents, maximum number of iterations, and salp population with considering of the binary bound of dimension
(2) Retain the search agents that satisfies all the constraints
(3) Run the load flow and evaluate the objective function using equation (7)
(4) Calculate the reliability indices of each bus
(5) Obtain the best salp position or leader salp position using equation (22)
(6) Update the value of C_1 using equation (23)
(7) Update the location of the leader using equation (22)
(8) Calculate the probabilities using equation (25) which take the output of equation (22) as an input to equation (26)
(9) Update the followers using equation (24)
(10) Check the program stopping condition, if *iteration* < *the maximum* number, go to step 6, otherwise go to step 11
(11) Print the optimal results
(12) End

Algorithm 1: The main steps of binary salp swarm algorithm (BSSA) [43].

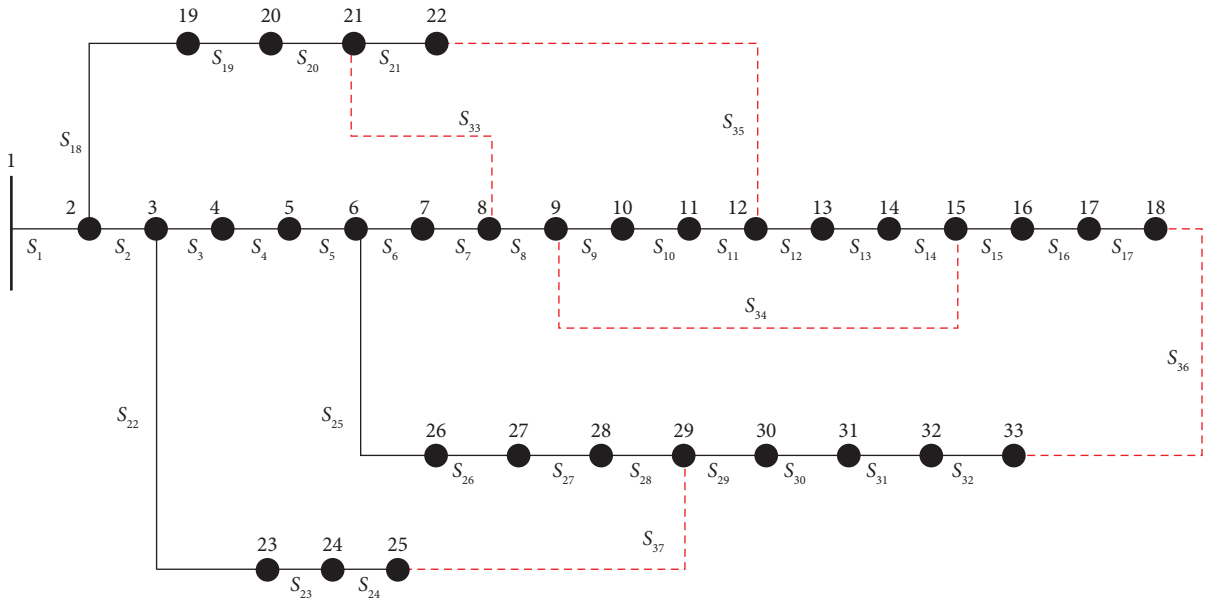

Figure 4: 33-bus IEEE system used in this work.

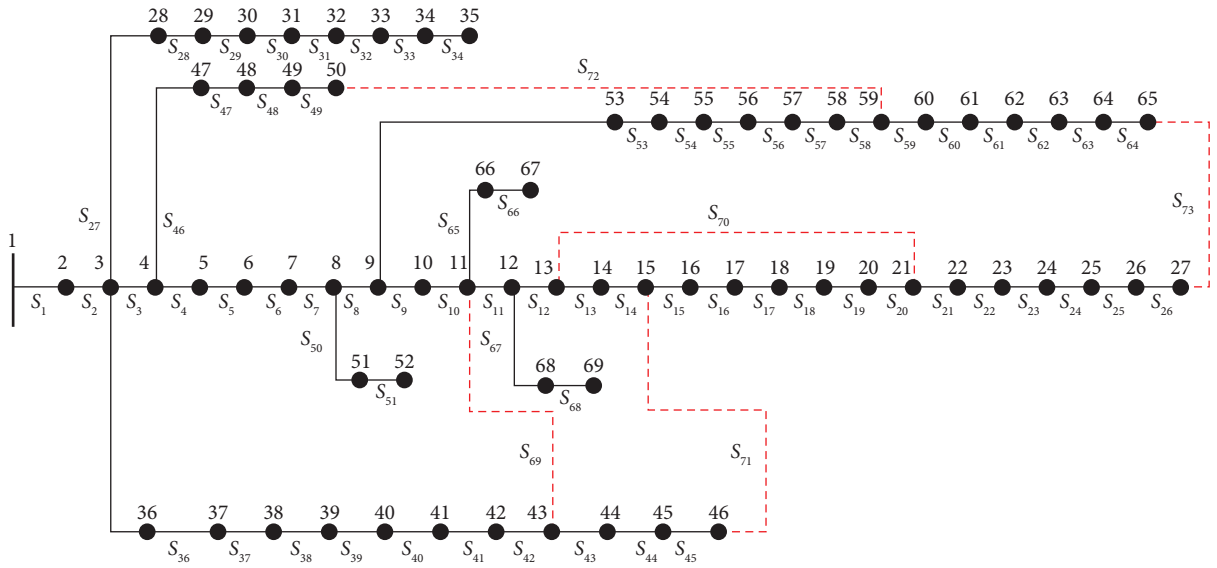

Figure 5: 69-bus IEEE system used in this work.

Table 1: The results and comparison among the scenarios for the IEEE 33-bus RSD.

Parameter	Scenarios			
	Base case	Sequentially COP after DSR	DSR after OCP	Simultaneously DSR and OCP
Tie switch number	33, 34, 35, 36, and 37	7, 14, 30, 35, and 37	11, 27, 33, 34, and 36	7, 11, 17, 34, and 37
Total power loss (kW)	202.6771	115.7382	105.9175	104.5116
Capacitor location	—	19, 23, and 30	6, 24, and 33	19, 30, and 33
Capacitor size KVAR	—	100, 600, and 100	600, 600, and 600	600, 600, and 600
V_{min} (p.u.)	0.91306	0.95	0.95	0.95732
V_{max} (p.u.)	1	1	1	1
Execution time (sec)	0.23802	391.1491	761.0816	789.1659
Convergence iterations	—	1	29	37
Percentage loss reduction	—	42.8953	47.7408	48.4344
SAIDI (hr/c.yr)	2.0436	1.7872	1.5424	1.5151
SAIFI (f/c.yr)	2.4126	2.2716	2.0964	2.0839
EENS (MWhr/yr)	2066.6446	1918.6544	1894.0194	1605.2589
AENS (MWhr/C.yr)	0.113550	0.105420	0.104070	0.088201
ASAI (p.u.)	0.99977	0.99981	0.99981	0.99984
CAIDI (hr/c.Int.)	0.84703	0.78675	0.73576	0.72703
ASUI (p.u.)	0.00023328	0.00019482	0.00018714	0.00015796

3.1. IEEE-33 Bus. The effects of adding OCP as well as changing the state of tie switches to build a new radial structure in the DSR on the test systems is examined in these three scenarios and described in Table 1, which calculates the main results of the proposed BSSA including the tie switches for these scenarios. Active power loss, capacitor location, capacitor size, reliability indices (SAIDI, SAIFI, EENS, AENS, ASAI, and CAIDI), minimum voltage, maximum voltage, and % loss reduction are listed in both tables. All these parameters have been improved in these scenarios from the base case for both test system.

The results of Table 1 indicate that the topology of RDS changes in each scenario according to the change of open tie switches. Figures 6–8 show the position and value of OCP, as well as the new structure of RDS after the optimization process.

The voltage profile is shown in Figure 9 using the BSSA for the test RDS under three scenarios with the base case, it offers a significant improvement in the voltage for all buses of the system, which contributes to increasing the efficiency of system.

The results obtained show a clear superiority of the technique that used in scenario 3, in term of losses reduced to 104.5116 kW, while keeping all RDS constraints within the permissible range. Figures 10 and 11 show the improvement in active and reactive losses for all buses of RDS in the three scenarios compared with the base case. Furthermore, Figure 12 reports the convergence of active losses using the suggested BSSA algorithm for three scenarios used in this work.

According to the results of Table 1, the simulation results indicate that the optimization process using BSSA

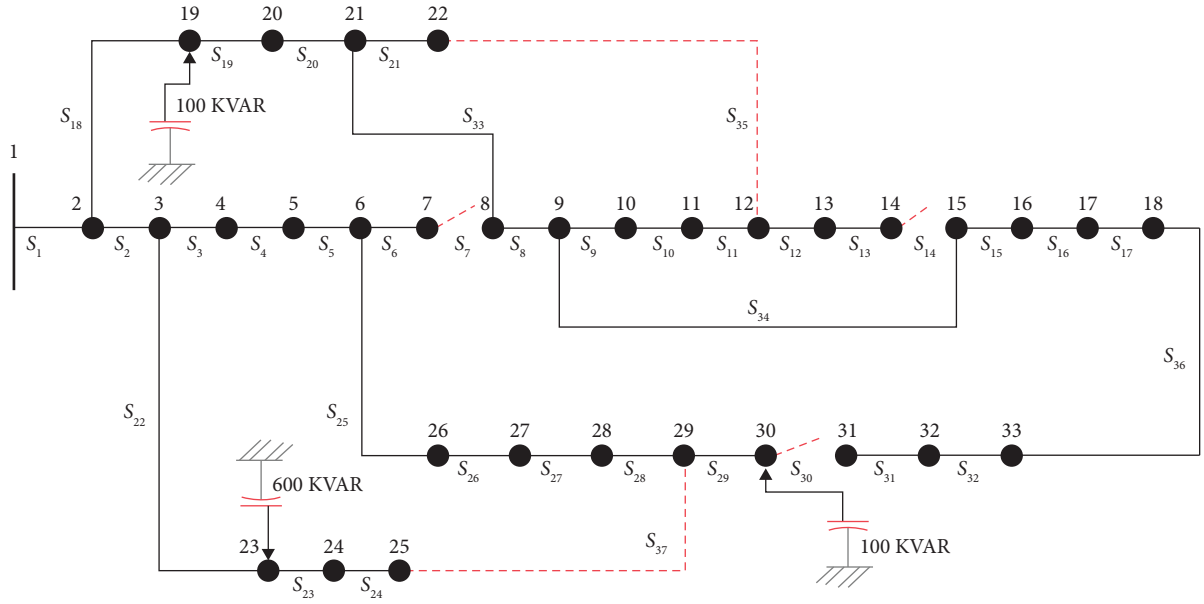

Figure 6: 33-bus IEEE system for scenario 1.

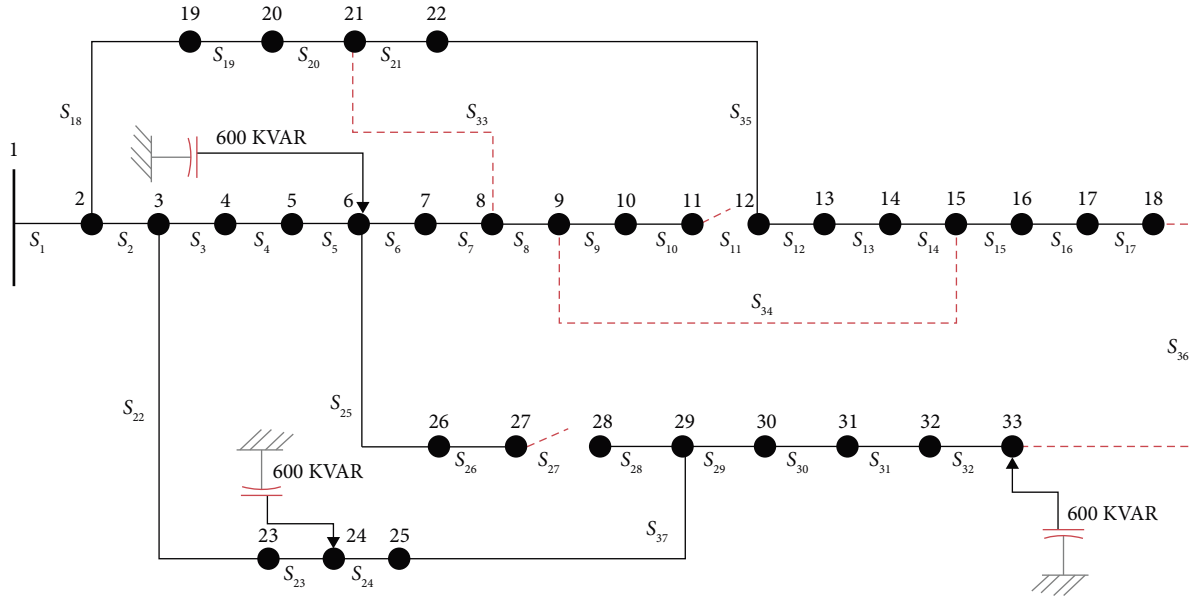

Figure 7: 33-bus IEEE system for scenario 2.

is successful in improvement the RDS reliability. By increasing the reserve of power supplied for consumers, the EENS and AENS indices will reduction for this reason. Detailed reliability analysis may also prevent the undesirable issues and minimize interruptions, hence then enhancing the power quality. The reliability indicators

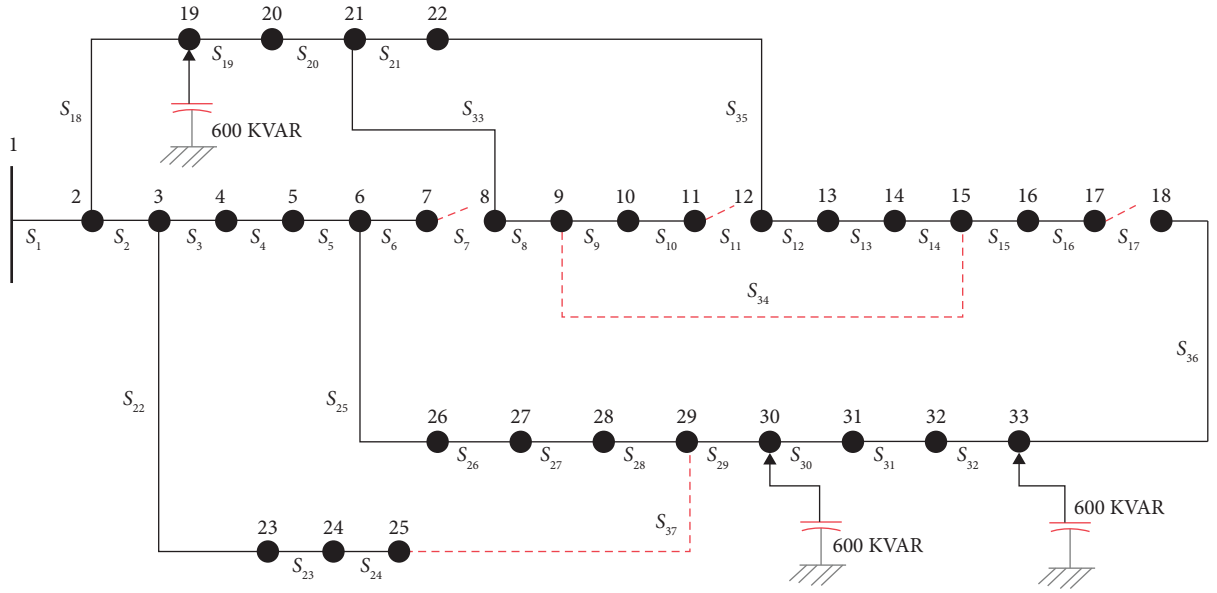

Figure 8: 33-bus IEEE system for scenario 3.

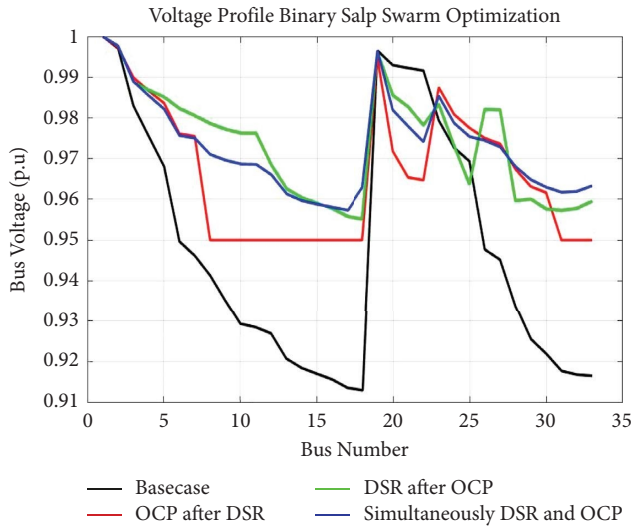

Figure 9: Voltage profile for 33-bus using BSSA algorithm for three scenarios with the base case.

that depend on the number of outages SAIDI, SAIFI, ASAI, CAIDI, and ASUI show a significant improvement from the base case.

Figure 13 shows the values of reliability indices studied in this paper after the optimization process with the base case. According to this figure, when comparing the three implemented scenarios, the best results are obtained for optimization in scenario 3, which outperforms both scenarios 1 and 2.

3.2. IEEE-69 Bus. The BSSA algorithm for 69-bus RDS is applied to perform another test to verify the success of techniques in the three proposed scenarios. To find out the

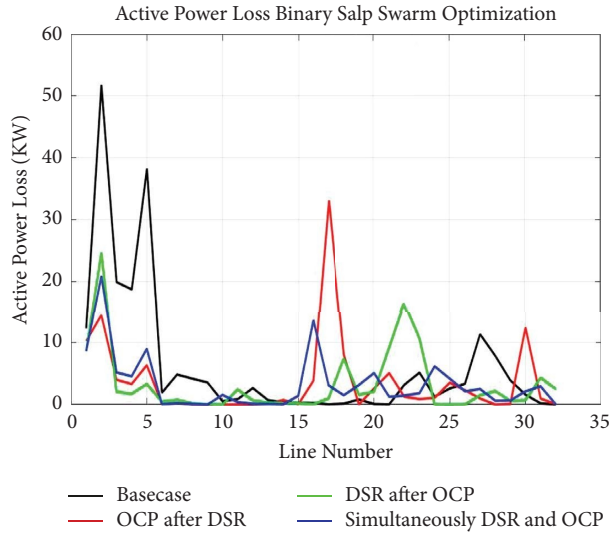

Figure 10: Active losses curve for 33-bus with using the BSSA algorithm for three scenarios with the base case.

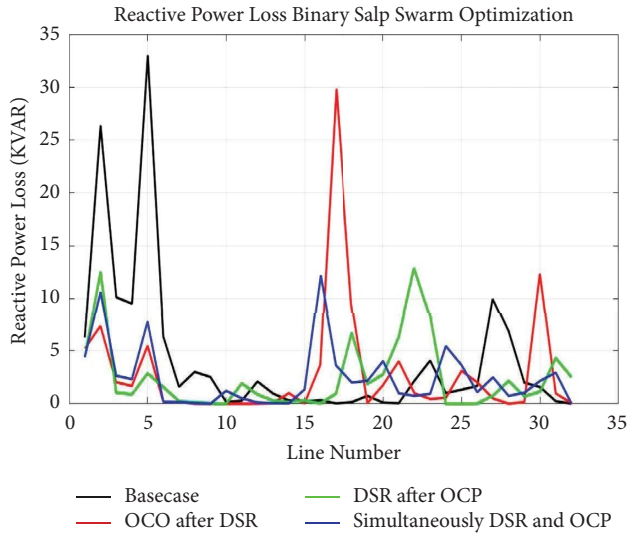

Figure 11: Reactive losses curve for 33-bus with using the BSSA algorithm for three scenarios with the base case.

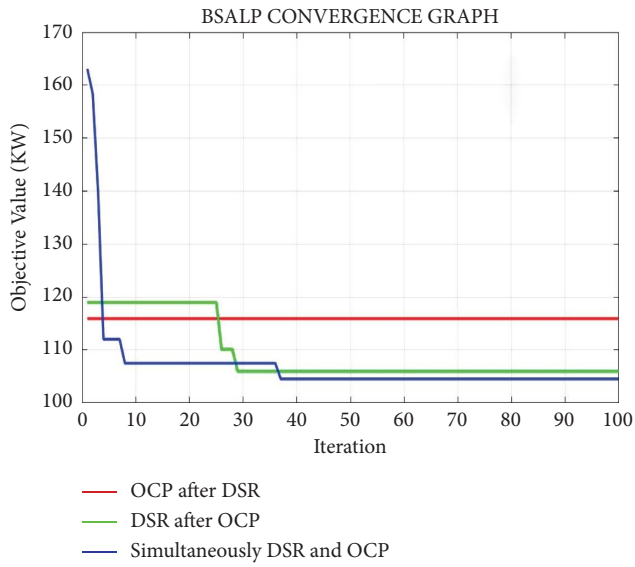

Figure 12: Convergence active power losses (kW) for 33-bus using the suggested BSSA algorithm.

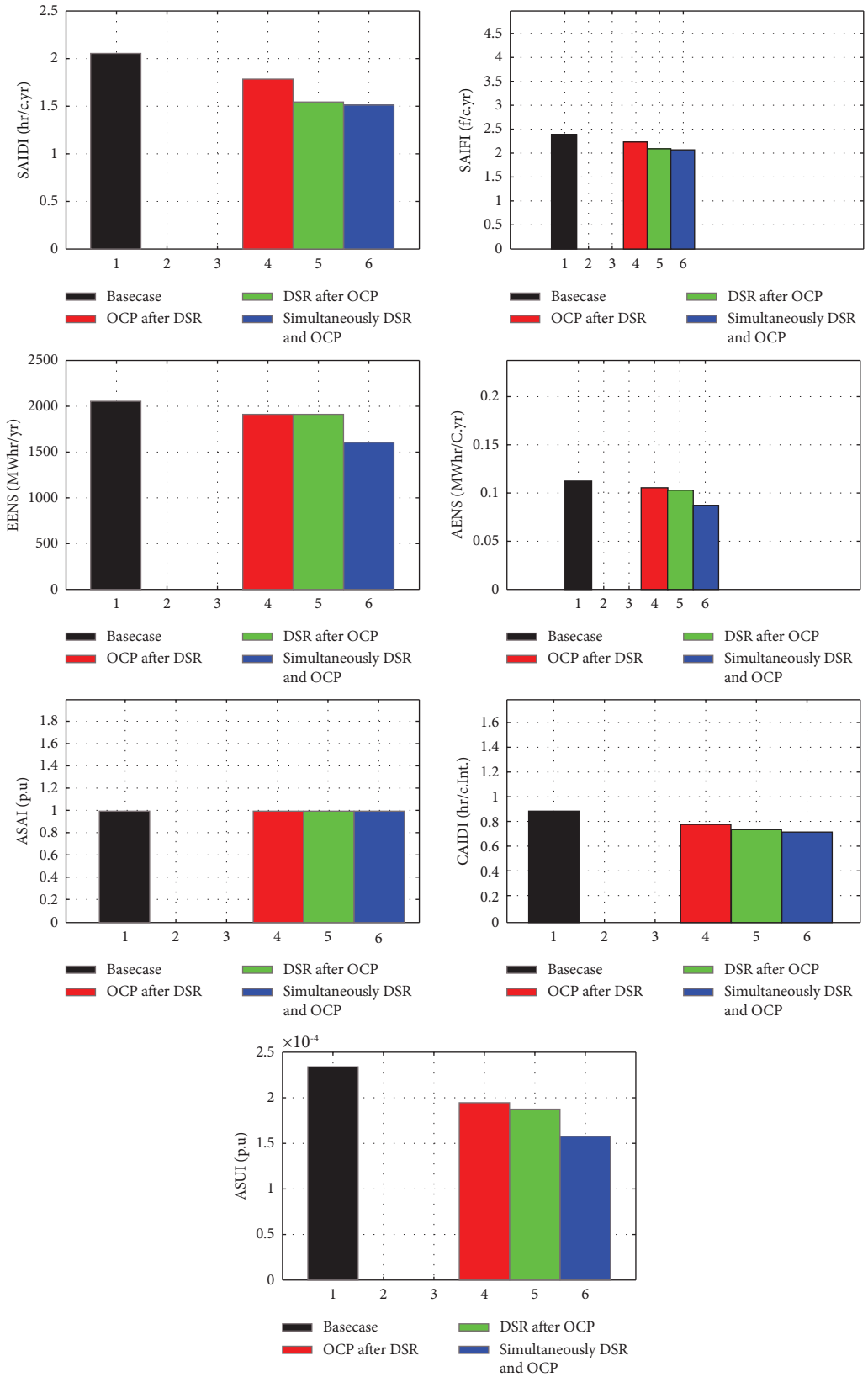

Figure 13: Reliability indices for 33-bus with using the BSSA algorithm for three scenarios with the base case.

Table 2: The results and comparison among the scenarios for the IEEE 69-bus RSD.

Parameter	Scenarios			
	Base case	Sequentially COP after DSR	DSR after OCP	Simultaneously DSR and OCP
Tie switch number	69, 70, 71, 72, and 73	16, 21, 40, 45, and 56	14, 42, 55, 62, and 70	14, 18, 38, 57, and 63
Total power loss (kW)	224.9606	95.2198	86.4039	85.4559
Capacitor location	—	28, 60, 66	15, 47, 60	39, 61, 65
Capacitor size KVAR	—	1200, 900, and 500	500, 1000, and 1000	700, 1100, and 500
V_{min} (p.u.)	0.90901	0.95	0.95	0.96632
V_{max} (p.u.)	1	1	1	1
Execution time (sec.)	1.7725	11390.2551	12383.004	18857.2237
Convergence iterations	—	49	37	6
Percentage loss reduction	—	57.6727	61.5915	62.0129
SAIDI (hr/c.yr)	1.00860	0.72352	0.71190	0.66594
SAIFI (f/c.yr)	1.5354	1.2797	1.2702	1.1240
EENS (MWhr/yr)	8.3287	3.6841	4.2457	3.5237
AENS (MWhr/C.yr)	0.00066897	0.00029591	0.00034102	0.00028303
ASAI (p.u.)	0.99988	0.99992	0.99992	0.99992
CAIDI (hr/c.Int.)	0.65691	0.6366	0.60427	0.58151
ASUI (p.u.)	0.00011514	8.2594×10^{-5}	8.1267×10^{-5}	7.6021×10^{-5}

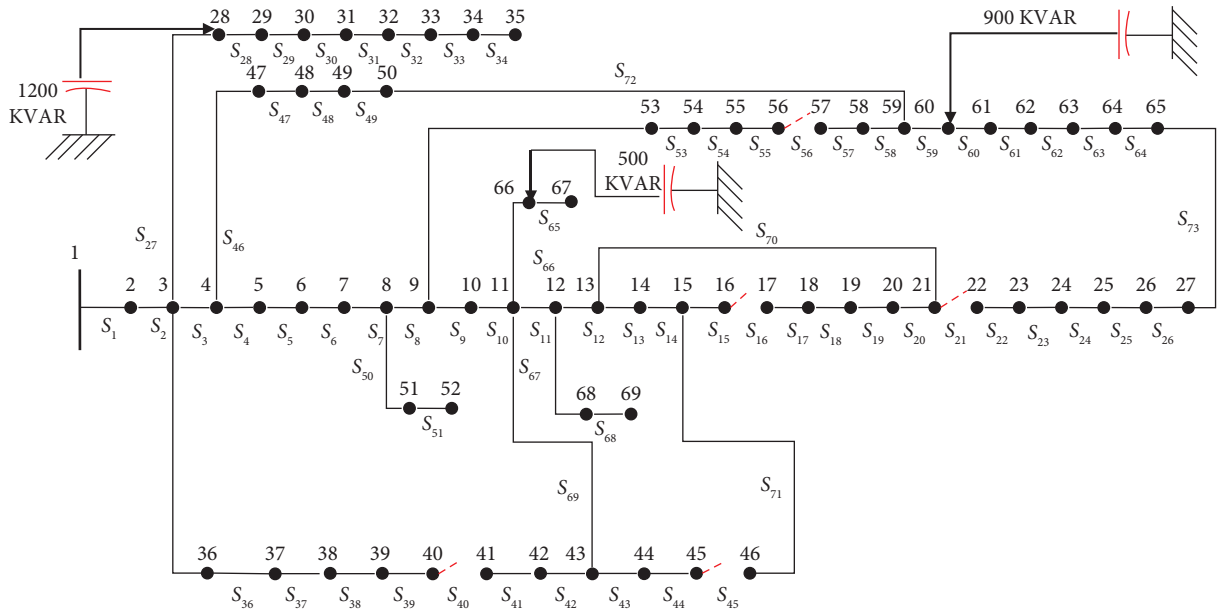

Figure 14: 69-bus IEEE system for scenario 1.

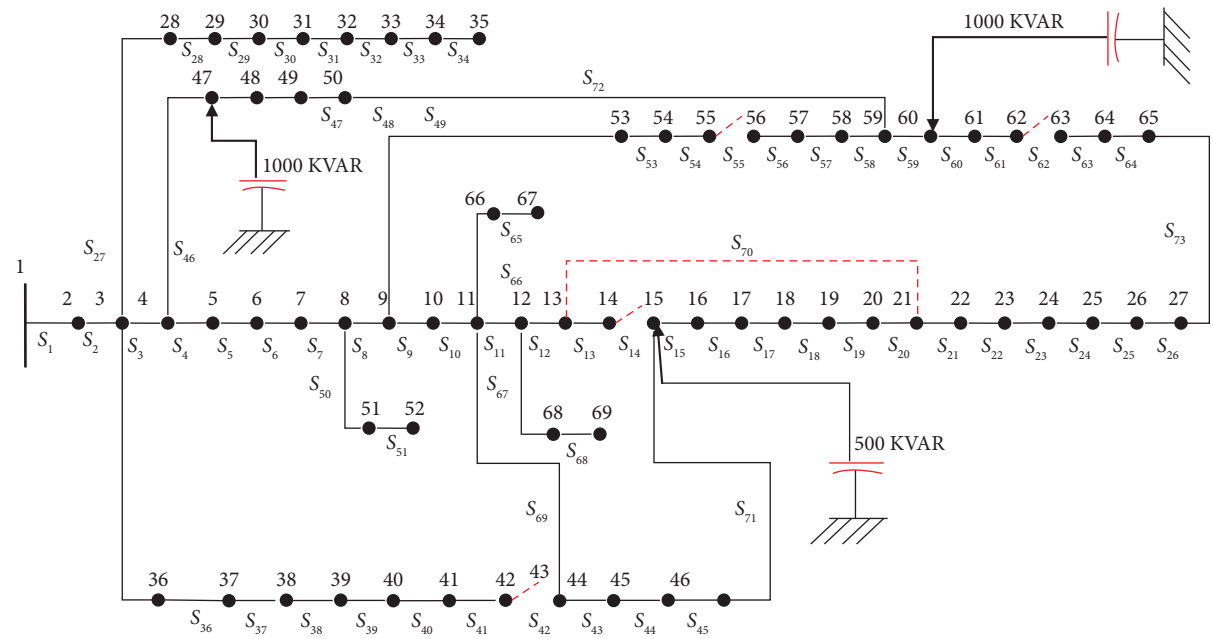

Figure 15: 69-bus IEEE system for scenario 2.

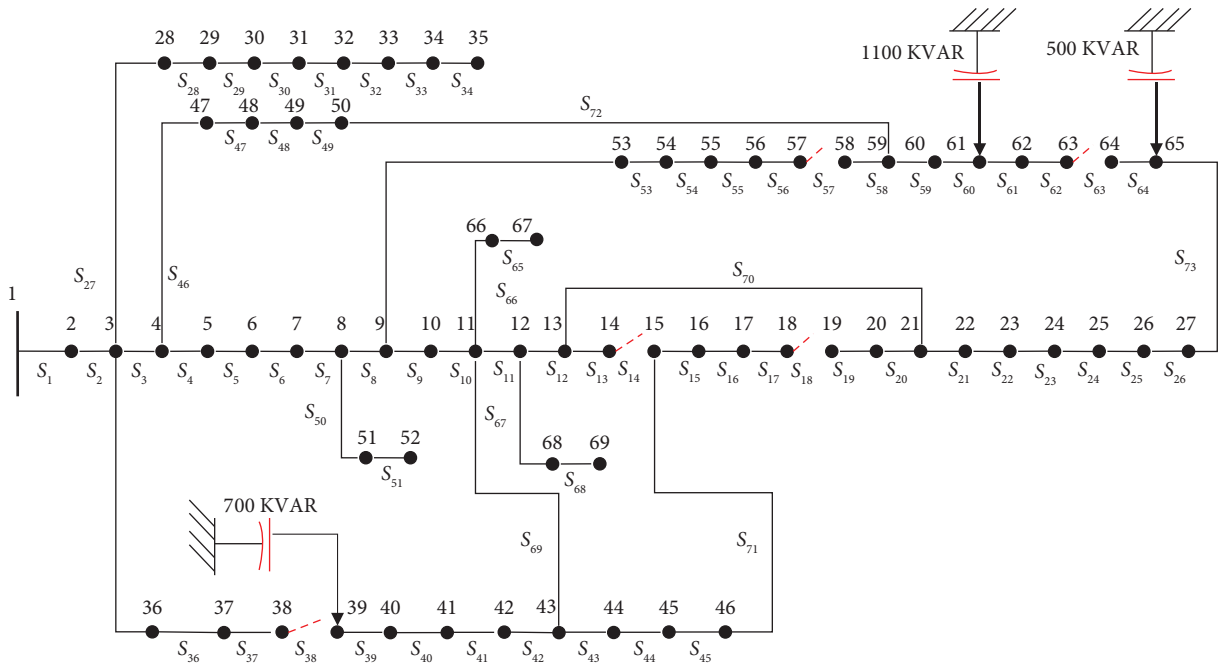

Figure 16: 69-bus IEEE system for scenario 3.

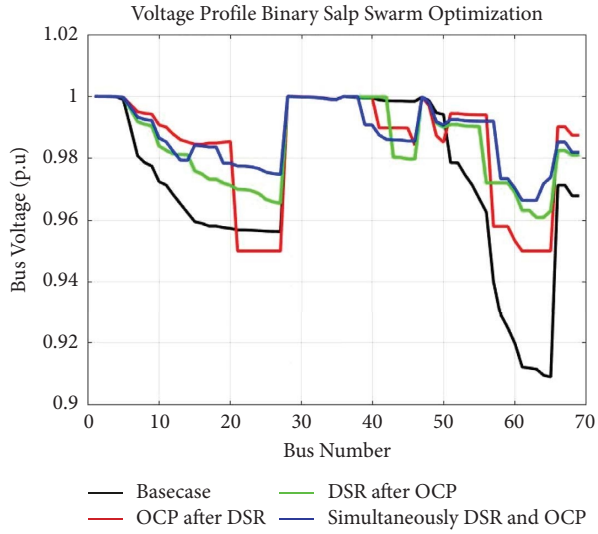

Figure 17: Voltage profile for 69-bus using BSSA algorithm for three scenarios with the base case.

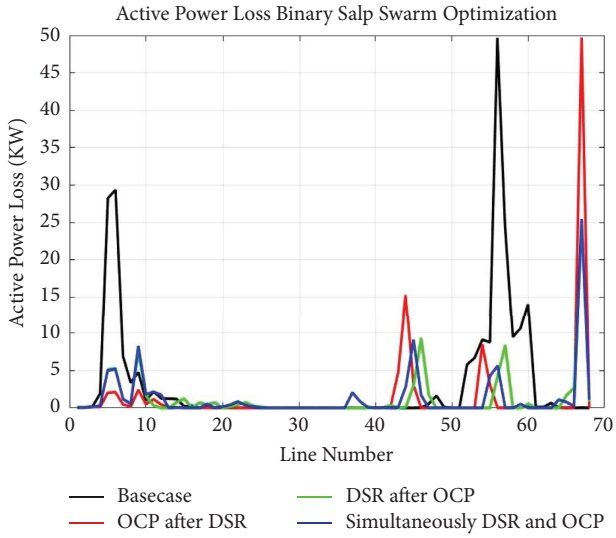

Figure 18: Active losses curve for 69-bus with using the BSSA algorithm for three scenarios with the base case.

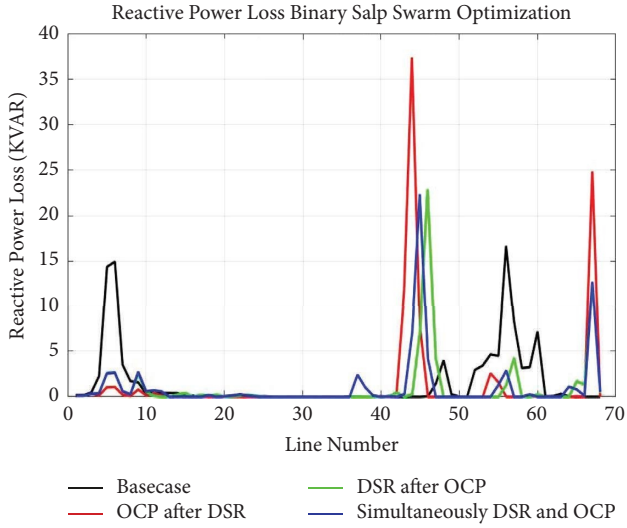

Figure 19: Reactive losses curve for 69-bus with using the BSSA algorithm for three scenarios with the base case.

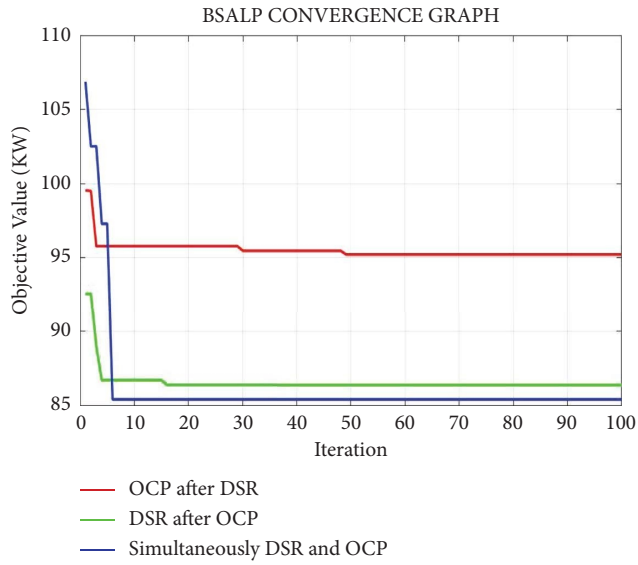

Figure 20: Convergence active power losses (kW) for 69-bus using the suggested BSSA algorithm.

effect of implementing the DSR technique and OCP technique sequentially or simultaneously for large distribution systems to improving the reliability and power quality. The results of three scenarios for the optimization process are listed in Table 2.

The results of Table 2 indicated that the radial topology of 69-bus RDS is changed in each scenario according to the change of the tie switches. Also, the places and values of injected capacitors differ in each scenario about the other. These differences are illustrated in the following Figures 14–16.

The voltage profile in Figure 17 shows a significant improvement in the three scenarios compared to the base case. The BSSA algorithm achieved significant success in optimizing the objective of the voltage profile function, whereby the voltages of all network buses were optimized. Improving the voltage of buses for RDS helps for reducing the voltage drop in all branches of the network and this contributes effectively to improving the losses reduction. Minimizing the active losses is the primary goal of this research, and the proposed algorithm has succeeded in finding the optimal radial structure of 69-bus RDS and the best values and locations of capacitors based on the OCP technique. These scenarios contributed for reducing the losses to the lowest possible value according to the established system constraints. Figure 18 shows the active power loss reduction in RDS for three scenarios with the base case where the scenario 3 shows superiority in reducing losses. Figure 19 shows the effect of KVAR compensation through OCP injection that contributes to reducing the reactive losses of the network compared to the base case.

The convergence of active losses using the suggested BSSA algorithm for three scenarios that used in this work is shown in Figure 20.

The simulation results of Table 2 indicate the success of the BSSA algorithm for maximizing the voltages of system buses with reducing losses in a balanced way, while improving the reliability of 69 RDS as a prerequisite for the optimization process. The reliability indices also show a significant improvement in the three scenarios compared with the base case. Figure 21 shows a comparison among the reliability indices for three scenarios.

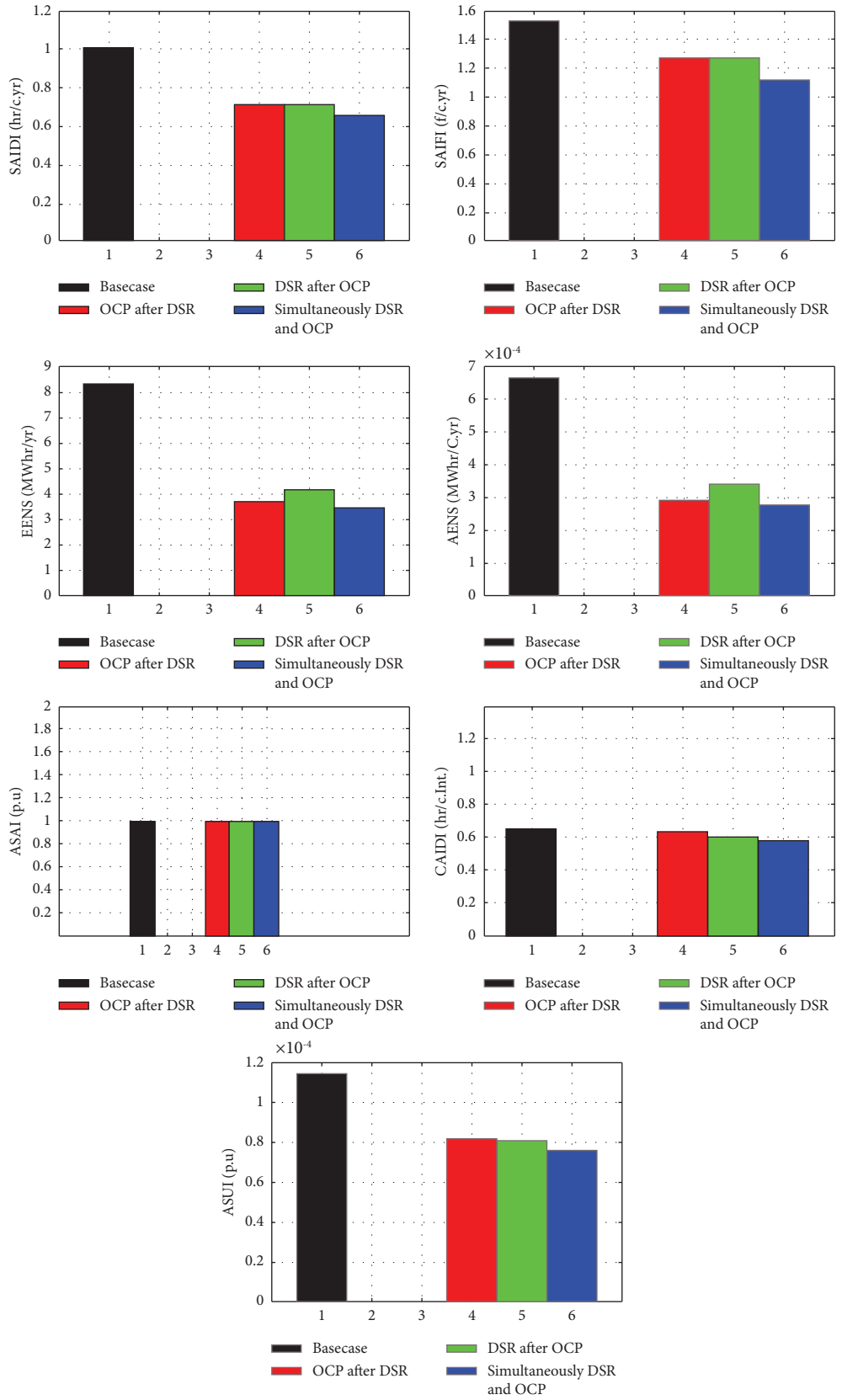

Figure 21: Reliability indices for 69-bus with using the BSSA algorithm for three scenarios with the base case.

4. Conclusions and Future Work

Several previous researches presented studies for improving the power quality of RDS by reducing the active losses and optimizing the system voltage profile without observance the system reliability concerns. So, a new method was devised to improve the power quality and reliability of RDS in an equiponderant manner to address these concerns. In this research, three different scenarios were used for 33 and 69 bus IEEE RDS, the first one OCP after DRS, the second DSR after OCP, and the third simultaneous DSR and OCP. The modern artificial intelligence algorithm, known as BSSA has been applied for these three scenarios to raise the reliability and performance of RDS by selecting the best locations and sizes of capacitors in addition to modifying the system topology. The main conclusions of this study are summarized as follows:

(1) The DSR and OCP techniques need a strong load flow method; therefore, backward/forward sweep load flow provides this capability due to its efficiency and speed when compared with NRM

(2) Simulation results expose the effectiveness and robustness of the proposed algorithm in implementing a MOF for reducing the system losses and amelioration the voltage profile in the three mentioned scenarios

(3) All RDS reliability indices are enhanced through three different optimization scenarios which can be helped for increasing the reserve power supplied to consumers and reducing the number of interruptions

(4) The optimal dual sequential and dual-simultaneous techniques (OCP after DRS, DSR after OCP, and simultaneous DSR and OCP) based on BSSA have been contributed successfully to improve the percentage of loss reduction in the three scenarios (42.8953%, 47.7408%, and 48.4344%), respectively, in 33-bus RDS and to (57.6727%, 61.5915%, and 62.0129%), respectively, in 69-bus RDS

(5) The dual-simultaneous technique (scenario 3) demonstrates its superiority over dual sequential techniques (scenarios 1 and 2) for improving the loss reduction, better voltage optimization, and a significant increase in the network reliability

Based on the results of this study, the following studies that can be addressed as a possible extension in the future:

(i) Kinds of disturbances might be applied to the system under study such as symmetrical three-phase fault, unsymmetrical faults, and switching failure

(ii) Achieve the improvement of loss reduction, voltage profile, and network reliability by using other dual sequential and dual-simultaneous techniques or optimization methods

Data Availability

The data supporting the results of this study are indicated in reference [37] in the manuscript.

Disclosure

The author Mohanad Muneer is a master's student at Middle Technical University, Electrical Engineering Technical College, Department of Electrical Power Engineering Techniques, Baghdad, Iraq.

Conflicts of Interest

The authors declare that they have no conflicts of interest regarding the publication of this paper.

Acknowledgments

This research was funded by the authors at their own expense.

References

[1] A. Tabares, G. Munoz-Delgado, J. F. Franco, J. M. Arroyo, and J. Contreras, "An enhanced algebraic approach for the analytical reliability assessment of distribution systems," *IEEE Transactions on Power Systems*, vol. 34, no. 4, pp. 2870–2879, 2019.

[2] M. Ghiasi, "Detailed study, multi-objective optimization, and design of an AC-DC smart microgrid with hybrid renewable energy resources," *Energy*, vol. 169, pp. 496–507, 2019.

[3] N. Gupta, A. Swarnkar, and K. R. Niazi, "Distribution network reconfiguration for power quality and reliability improvement using Genetic Algorithms," *International Journal of Electrical Power & Energy Systems*, vol. 54, pp. 664–671, 2014.

[4] A. Shaheen, A. Elsayed, A. Ginidi, R. El-Sehiemy, and E. Elattar, "Reconfiguration of electrical distribution network-based DG and capacitors allocations using artificial ecosystem optimizer: practical case study," *Alexandria Engineering Journal*, vol. 61, no. 8, pp. 6105–6118, August 2022.

[5] D. Esmaeili, K. Zare, B. M. Ivatloo, and S. Nojavan, "Simultaneous optimal network reconfiguration, DG and fixed/switched capacitor banks placement in distribution systems using dedicated genetic algorithm," *Majlesi Journal of Electrical Engineering*, vol. 9, no. 4, pp. 31–41, 2015.

[6] A. N. Hussain, W. K. Shakir Al-Jubori, and H. F. Kadom, "Hybrid design of optimal capacitor placement and reconfiguration for performance improvement in a radial distribution system," *Journal of Engineering*, vol. 2019, Article ID 1696347, pp. 1-15, 2019.

[7] K. Prakash and M. Sydulu, "Particle Swarm Optimization Based Capacitor Placement on Radial Distribution Systems," in *Proceedings of the 2007 IEEE Power Engineering Society General Meeting*, pp. 1–5, Tampa, FL, USA, June 2007.

[8] A. H. Etemadi and M. Fotuhi-Firuzabad, "Distribution system reliability enhancement using optimal capacitor placement," *IET Generation, Transmission & Distribution*, vol. 2, no. 5, pp. 621–631, 2008.

[9] G. Srinivasan, "Optimization of distributed generation units in reactive power compensated reconfigured distribution network," *Automatika*, vol. 62, no. 2, pp. 249–263, 2021.

[10] W. K. Shakir Al-Jubori and A. N. Hussain, "Optimum reactive power compensation for distribution system using dolphin algorithm considering different load models," *International Journal of Electrical and Computer Engineering*, vol. 10, no. 5, p. 5032, May 2020.

[11] M. Fathi and M. Ghiasi, "Optimal DG placement to find optimal voltage profile considering minimum DG investment cost in smart neighborhood," *Smart Cities*, vol. 2, no. 2, pp. 328–344, June 2019.

[12] M. Ghiasi, T. Niknam, M. Dehghani, P. Siano, H. Haes Alhelou, and A. Al-Hinai, "Optimal multi-operation energy management in smart microgrids in the presence of RESs based on multi-objective improved DE algorithm: cost-emission based optimization," *Applied Sciences*, vol. 11, no. 8, pp. 3661–3728, 2021.

[13] E. S. Ali, S. M. Abd Elazim, and A. Y. Abdelaziz, "Optimal allocation and sizing of renewable distributed generation using ant lion optimization algorithm," *Electrical Engineering*, vol. 100, no. 1, pp. 99–109, 2018.

[14] M. Ghiasi and J. Olamaei, "Optimal capacitor placement to minimizing cost and power loss in tehran metro power distribution system using ETAP (A case study)," *Complexity*, vol. 21, no. S2, pp. 483–493, 2016.

[15] A. Y. Abdelaziz, E. S. Ali, and S. M. Abd Elazim, "Flower pollination algorithm for optimal capacitor placement and sizing in distribution systems," *Electric Power Components and Systems*, vol. 44, no. 5, pp. 544–555, 2016.

[16] A. Roosta, H. R. Eskandari, and M. H. Khooban, "Optimization of radial unbalanced distribution networks in the presence of distribution generation units by network reconfiguration using harmony search algorithm," *Neural Computing and Applications*, vol. 31, no. 11, pp. 7095–7109, 2018.

[17] S. Das, D. Das, and A. Patra, "Reconfiguration of distribution networks with optimal placement of distributed generations in the presence of remote voltage controlled bus," *Renewable and Sustainable Energy Reviews*, vol. 73, pp. 772–781, 2017.

[18] S. M. A. Elazim and E. S. Ali, "Optimal network restructure via improved whale optimization approach," *International Journal of Communication Systems*, vol. 34, no. 1, pp. 1–15, 2020.

[19] R. D. Mohammedi, R. Zine, M. Mosbah, and S. Arif, "Optimum network reconfiguration using grey wolf optimizer," *TELKOMNIKA (Telecommunication Computing Electronics and Control)*, vol. 16, no. 5, pp. 2428–2435, 2018.

[20] H. B. Duan, G. J. Ma, and D. L. Luo, "Optimal formation reconfiguration control of multiple UCAVs using improved particle swarm optimization," *Journal of Bionics Engineering*, vol. 5, no. 4, pp. 340–347, 2008.

[21] G. Namachivayam, C. Sankaralingam, S. K. Perumal, and S. T. Devanathan, "Reconfiguration and capacitor placement of radial distribution systems by modified flower pollination algorithm," *Electric Power Components and Systems*, vol. 44, no. 13, pp. 1492–1502, 2016.

[22] R. Av Sudhakara and R. M. Damodar, "Application of whale optimization algorithm for distribution feeder reconfiguration," *imanager's Journal on Electrical Engineering*, vol. 11, no. 3, pp. 17–24, 2018.

[23] A. A. Z. Diab and H. Rezk, "Optimal sizing and placement of capacitors in radial distribution systems based on grey wolf, dragonfly and moth–flame optimization algorithms," *Iranian Journal of Science and Technology, Transactions of Electrical Engineering*, vol. 43, no. 1, pp. 77–96, 2018.

[24] S. Chakrabarti, G. Ledwich, and A. Ghosh, "Reliability driven reconfiguration of rural power distribution systems," in *Proceedings of the 2009 International Conference on Power Systems*, pp. 1–6, Kharagpur, India, April 2010.

[25] M. Sedighizadeh, M. Dakhem, M. Sarvi, and H. H. Kordkheili, "Optimal reconfiguration and capacitor placement for power loss reduction of distribution system using improved binary particle swarm optimization," *International Journal of Energy and Environmental Engineering*, vol. 5, no. 1, pp. 73–11, 2014.

[26] A. V. S. Reddy and Dr. M. D. Reddy, "Optimal capacitor allocation for the reconfigured network using ant lion optimization," *International Journal of Applied Engineering Research ISSN*, vol. 12, no. 12, pp. 3084–3089, 2017.

[27] L. A. Gallego, J. M. Lopez-Lezama, and O. G. Carmona, "A mixed-integer linear programming model for simultaneous optimal reconfiguration and optimal placement of capacitor banks in distribution networks," *IEEE Access*, vol. 10, pp. 52655–52673, 2022.

[28] V. Tamilselvan, T. Jayabarathi, T. Raghunathan, and X. S. Yang, "Optimal capacitor placement in radial distribution systems using flower pollination algorithm," *Alexandria Engineering Journal*, vol. 57, no. 4, pp. 2775–2786, 2018.

[29] K. S. Kumar and T. Jayabarathi, "Power system reconfiguration and loss minimization for an distribution systems using bacterial foraging optimization algorithm," *International Journal of Electrical Power & Energy Systems*, vol. 36, no. 1, pp. 13–17, 2016.

[30] T. Thakur and J. Dhiman, "A new approach to load flow solutions for radial distribution system," in *Proceedings of the 2006 IEEE/PES Transmission & Distribution Conference and Exposition: Latin America*, pp. 1–6, Caracas, Venezuela, April 2006.

[31] S. Ouali and A. Cherkaoui, "An improved backward/forward sweep power flow method based on a new network information organization for radial distribution systems," *Journal of Electrical and Computer Engineering*, vol. 2020, Article ID 5643410, 11 pages, 2020.

[32] H. F. Kadom, A. N. Hussain, and W. K. S. Al-Jubori, "Dual technique of reconfiguration and capacitor placement for distribution system," *International Journal of Electrical and Computer Engineering*, vol. 10, no. 1, pp. 80–90, 2020.

[33] T. Hongxun, Y. Rong, and Z. Yuan, "Computation of probability distribution for reliability indices of distribution system containing distributed generation," *Power System Technology*, vol. 37, no. 6, pp. 1562–1569, 2013.

[34] M. A. Gana, U. O. Aliyu, and G. A. Bakare, "Evaluation of the reliability of distribution system with distributed generation using ETAP," *ABUAD Journal of Engineering Research and Development*, vol. 2, no. 1, pp. 103–110, 2019.

[35] L. jikeng, W. Xudong, and Q. Ling, "Reliability evaluation for the distribution system with distributed generation," *European Transactions on Electrical Power*, vol. 21, no. 1, pp. 895–909, 2010.

[36] A. Abdukhakimov, S. Bhardwaj, G. Gashema, and D. S. Kim, "Reliability analysis in smart grid networks considering distributed energy resources and storage devices," *International Journal of Electrical and Electronic Engineering & Telecommunications*, vol. 8, no. 5, pp. 233–237, 2019.

[37] G. S. Kumar, S. S. Kumar, and S. V. J. Kumar, "DG placement using loss sensitivity factor method for loss reduction and reliability improvement in distribution system," *International Journal of Engineering & Technology*, vol. 7, pp. 236–240, 2018.

[38] P. Jahangiri and M. F. Firuzabad, "Reliability Assessment of Distribution System with Distributed Generation," in *Proceedings of the 2008 IEEE 2nd International Power And Energy Conference*, pp. 1551–1556, Johor Bahru, Malaysia, December 2008.

[39] A. O. Salau, Y. W. Gebru, and D. Bitew, "Optimal network reconfiguration for power loss minimization and voltage

profile enhancement in distribution systems," *Heliyon*, vol. 6, no. 6, e04233 pages, June 2020.

[40] S. Mirjalili, A. H. Gandomi, S. Z. Mirjalili, S. Saremi, H. Faris, and S. M. Mirjalili, "Salp Swarm Algorithm: a bio-inspired optimizer for engineering design problems," *Advances in Engineering Software*, vol. 114, pp. 163–191, 2017.

[41] M. Khamees, A. S. Albakry, and K. D. Shaker, "A new approach for features selection based on binary salp swarm algorithm," *Journal of Theoretical and Applied Information Technology*, vol. 96, no. 7, 2018.

[42] R. M. Rizk-Allah, A. E. Hassanien, M. Elhoseny, and M. Gunasekaran, "A new binary salp swarm algorithm: development and application for optimization tasks," *Neural Computing & Applications*, vol. 31, no. 5, pp. 1641–1663, 2018.

[43] H. Faris, M. M. Mafarja, A. A. Heidari et al., "An efficient binary Salp Swarm Algorithm with crossover scheme for feature selection problems," *Knowledge-Based Systems*, vol. 154, no. 15, pp. 43–67, 2018.